www.amlett.com, www.amlett.org, DOI: 10.5185/amlett.2013.8541 Published online by the VBRI press in 2014

Synthesis of air stable copper nanoparticles and their use in catalysis

Razium Ali Soomro[1*], Syed Tufail Hussain Sherazi[1], Sirajuddin[1], Najma Memon[1], Mohammad Raza Shah[2], Nazar Hussain Kalwar[1], Keith Richard Hallam[3], Afzal Shah[4]

[1]*National Centre of Excellence in Analytical Chemistry, University of Sindh, Jamshoro 76080, Pakistan*
[2]*International Centre for Chemical and Biological Sciences, HEJ Research Institute of Chemistry University of Karachi, Pakistan*
[3]*Interface Analysis Centre, School of Physics, University of Bristol, Bristol, BS8 1TL, United Kingdom*
[4]*Department of Chemistry, University of Science & Technology, Bannu 28100, Khyber Pakhtunkhwa, Pakistan*

[*]Corresponding author. Tel: (+92) 3363051253; E-mail: raziumsoomro@gmail.com

Received: 26 August 2013, Revised: 29 September 2013 and Accepted: 18 October 2013

ABSTRACT

The undertaken study describes synthesis of air resistant copper nanoparticles (Cu NPs) in an aqueous phase using sodium borohydride as a reducing agent via chemical reduction method. The hydrosol has resistant to oxidation by atmospheric oxygen for several days. The air stability was induced by capping Cu NPs with anionic surfactant "sodium dodecyl sulfate (SDS)". Ascorbic acid was used as an antioxidant. These Cu NPs were characterized by ultraviolet-visible (UV-VIS) spectroscopy, which contributed towards the understanding of surface plasmon resonance (SPR) generation and optical behavior of Cu NPs. It was used as an optical tracer for size control and confirmation of Cu NPs and was found to be affected by various parameters like reaction time, pH, concentration of copper sulfate and the surfactant SDS. SPR peaks were found to shift from 597 to 569 nm, while apparent color changes from yellow to brick red. Further characterization studies were carried out by using fourier transform infrared (FT-IR) spectroscopy to investigate the co-ordination between Cu NPs and SDS. X-ray diffraction (XRD) was used for phase purity of Cu NPs. Transmission electron microscopy (TEM) and atomic force microscopy (AFM) were used the size and morphological characterization. The average size of the Cu NPs was found to be 15 nm in diameter with an average height of 14 nm. The Cu NPs showed excellent catalytic activity in the reductive degradation of Eosin B (EB) dye in just 16 sec of reaction time and maintained their catalytic activity when reused multiple times. The degradation rate was found to follow first order reaction kinetics with the EB degradation. The Cu NPs enhanced the rate of EB degradation 30 times more than the control test. Copper was found an attractive catalyst in the nanosize regimes. The Cu NPs are more economical as compared to noble metals. The Cu NPs are expected to be suitable alternative and play an imperative role in the fields of catalysis and environmental remediation.

Keywords: Copper nanoparticles; sodium dodecyl sulfate; eosin B; nanocatalysts.

Razium Ali Soomro is a Ph.D. research scholar at National Centre of Excellence in Analytical Chemistry (NCEAC), University of Sindh, Jamshoro, Pakistan. He is working on the synthesis of metal nanoparticles and their applications.

Syed Tufail Hussain Sherazi received his Ph.D. in the field of analytical chemistry at NCEAC, University of Sindh, Jamshoro, Pakistan in 1997. He did Post Doctorate in Food Science Department from McGill University Canada in 2006. He worked as Chief Chemist, Agro Oil Extraction Ltd., Dera Ismail Khan and as Research Officer at Gomal University Dera Ismail Khan (NWFP), Pakistan. He was then Production Manager in SS Oil Mill Vehari, Pakistan. He is the member of Chemical Society of Pakistan, American Oil Chemists Society (AOCS) and National Representative IUPAC Division of Chemistry and Environment. He is Professor at NCEAC, University of Sindh, Jamshoro, Pakistan. His research interests include Nanomaterials synthesis and their use in catalysis. His especial interest is in the composition of edible oils and their role in human nutrition (Lipid Chemistry). He is also interested in the detection and quantification of mycotoxins in poultry feed by FT-IR spectroscopy.

Sirajuddin received his Ph.D. in the field of electrochemistry from University of Peshawar, Khyber Puktoonkhwa, Pakistan in 1999. He did his postdoctoral research work at Monash University, Clayton (Melbourne) Australia in 2007. He is the member of Chemical Society of Pakistan, Microscopy Society of Pakistan and Material Research Society of Pakistan. He is working as professor at NCEAC, University of Sindh, Jamshoro, Pakistan. His field of interest includes the synthesis and application of nanoparticles in sensors and catalysis and method development in various analytical techniques.

Introduction

Research in nanomaterials has achieved considerable attention because of their unique properties and numerous applications different areas **[1-2]**. Applications of such materials in different fields depend on the type and nature of nanoparticles (NPs). Metallic nanoparticles are of great interest due to their excellent chemical, physical and catalytic properties **[3]**. Among the metal nanoparticles, Cu NPs have received considerable public interest, which may be due to their good optical, electrical and thermal properties. Cu NPs were assumed cost-effective as compared to noble metals like Ag, Au, and Pt. Hence, they are potentially applied in the fields of catalysis **[4]**, cooling fluids **[5]** and conductive inks **[6]**. Due to plasmon surface resonance, Cu NPs exhibit enhanced nonlinear optical properties, which allowed wide applications in optical devices and nonlinear optical materials, such as optical switches or photo chromic glasses **[3**,**7**,**8]**.

It is evident from the previously reported studies that perspective developments in the synthesis of Cu NPs are very significant tasks other than their applications in various fields. Various methods like radiation **[9]**, micro-emulsion **[10]**, thermal decomposition **[11]**, and aqueous chemical reduction **[12]** have been applied for the synthesis of Cu NPs. The aqueous reduction method is widely selected for the synthesis of Cu NPs because it is robust, cost effective, efficient in yield, and requires limited equipment. It has simple control on the size and distribution of particles under controlled parameters, like concentration of precursor salt, capping agent and pH of solution **[13-16]**. However, Cu NPs in aqueous environment are largely prone to oxidation. The inevitably generation of surface oxide layers (Cu-oxides) was thermodynamically considered more stable as compared to pure Cu metal. Moreover, it was also noticed that copper particles form aggregates without proper protection. Such problems like aggregation and oxidation can be overcome by employing various protecting agents, such as polymers **[17**, **18]** and organic ligands **[19**, **20]**.

The synthesis of Cu NPs in an aqueous solution under nitrogen environment has been reported by some researchers **[21]**. While, formation of Cu NPs in non-aqueous environment using PVP polymer as a capping agent has also been suggested **[22]**. Some other methods **[10**, **23]** have also been proposed for the synthesis of Cu NPs using bis (ethylhexyl) hydrogen phosphate (HDEHP) in organic phase to prevent oxidation and KHB_4 as reducing agent and PEG-4000 as a protecting agent respectively. Most of the aforementioned procedures employ an oxygen-free atmosphere and heavy molecular weight polymers as protecting agent to prevent oxidation and aggregation of Cu NPs. Hence, it limits the use Cu NPs in an open environment and restrains the catalytic activity as most of active sites of the particles are blocked by heavy polymer chains.

Comparatively Cu NPs have wide range of applications than traditional catalysts because copper has low cost, easy availability, soft reaction conditions to produces high yields in less reaction time. The Cu NPs have also been reported as suitable heterogeneous recyclable catalyst in various environmental problems like hazardous wastes and toxic water pollutants **[3]**. Most of the recent studies on removing toxic pollutants from water system have focused on noble metals and their nano-particles **[24-27]**. With the growing interest in the textile industry and its waste effluents, in particular dye-containing waste water and their industrial discharge was reported as one of the major sources of water pollution worldwide **[25**, **28**, **29]**. The release of these colored effluents into aquatic systems is of environmental concern due to their carcinogenic properties, persistence and recalcitrant nature. Dyes released in waste water may also undergo anaerobic degradation, but incomplete breakdown of dyes by bacteria results in toxic products which are mutagenic to aquatic ecosystem. The less sunlight penetration and oxygen dissolution in colored waste water poses a considerable threat to marine life **[30]**. A number of biological and physico-chemical approaches have been introduced for the removal of dyes from aqueous media, including biological degradation, adsorption techniques, coagulation processes, hypochlorite treatment and ozonation methods **[31]**. However, some available reports demonstrate that such approaches are inefficient, expensive, require more effort and also result in secondary waste products, which may need further treatments **[32]**. The advanced oxidation processes (AOPs) employing photo-assisted reactions have been widely exploited for the degradation of azo dyes **[33-35]**. The comparative effectiveness of such processes results from the generation of highly reactive hydroxyl radicals which decolorize soluble and insoluble dyes. However, a major demerit of the method is generation of large volumes of iron sludge **[33]**. The use of titanium dioxide (TiO_2) for remediation of dyes is also a technically practicable clean-up approach but the requirement for UV light and low quantum yields hinder the general use of TiO_2 in practical remediation methodologies **[36**, **37]**.

The processes of advance degradation and multistep treatment were described to a significant level in practical applications **[38]**. Among such methodologies, reductive degradation of organic dyes with metal nanoparticles provides an economic, fast, efficient and convenient model system for biodegradation of the end products, like aromatic amine, which is readily and easily degraded by micro-organisms **[36**, **37**, **39]**. The spherical cysteine-derived gold nanoparticles (Cyst-Au NPs) show highly efficient catalytic reduction of dyes like Methylene Blue (MB), in the presence of $NaBH_4$ **[27]**. Similarly highly efficient nickel nanoparticles (Ni NPs) obtained by a wet chemical approach in an aqueous medium were employed for the complete degradation of Congo Red dye in a 50 sec reaction time **[40]**.

Many other scientists have also studied the reduction/degradation of dyes using different nanoscale metal particles for complete remediation of toxic dyes **[26**, **41**, **42]**. Although various studies have been performed using nanoscale noble metal particles like Au, Ag, Pd, and Pt, for high catalytic dye degradation yields **[9**, **10**, **24]**. The use of Cu NPs for degradation of dye stuffs has remained an unexplored area. Noticeably, very few reports have been published which demonstrate the synthesis of air durable Cu NPs and the use of SDS in controlling the size and morphology of these nanoparticles via aqueous reduction route **[33]**.

The undertaken study is novel and has not been reported earlier. It was aimed to develop a sensitive, robust, cost effective and environmental friendly method for the synthesis of Cu NPs and their applications as catalysts. The developed method focused on the synthesis of oxidation resistant and stable Cu NPs with narrow size and homogenous distribution in aqueous solution. A simple, inexpensive and easy chemical approach without any protective gas was applied for the production of Cu NPs. The study also highlights the SPR control of Cu NPs with various experimental parameters and corresponding color changes of colloidal Cu nano sol. Furthermore, these nanoparticles were applied as heterogeneous recyclable catalysts for efficient multiple degradation of EB (model hazardous compound).

Experimental

Materials

For the present work, we used analytical grade chemicals such as copper chloride pentahydrate ($CuCl_2$•$5H_2O$ - 97%), sodium dodecylsulphate (SDS - 98%), ascorbic acid (Vit-C - 98%) purchased from E. Merck and sodium borohydride ($NaBH_4$ - 98%), sodium hydroxide (NaOH - 98%), hydrochloric acid (HCl - 37%) obtained from Sigma-Aldrich, USA. All chemicals were used as-received without further purification.

Method of synthesis of Cu NPs

In a typical synthetic procedure Cu NPs were obtained via a modified wet chemical reduction route. This new procedure for Cu NPs fabrication was a simple process. 0.2 mL of 0.03 M $CuCl_2$•$5H_2O$ solution was diluted up to 5 mL with deionized water and got a blue color solution. Then, (1.0 mL of 1.0 M SDS) and (0.1 mL of 0.1 M Vitamin C) were mixed with the blue colored solution followed by further addition of the reducing agent (0.3 mL of 0.01 M $NaBH_4$), the solution was further diluted with deionized water and finally a 10 mL solution was obtained. With the passage of time, the color of the solution gradually changed from faint yellow to brick red with a number of intermediate stages. The appearance of the yellow/orange color indicated that the reduction reaction had initiated. The mechanism for reduction of Cu^{2+} to zero-valant Cu particles with $NaBH_4$ is given in reaction (1);

$$Cu^{2+} + 2BH_4^- \rightarrow Cu + H_2 + B_2H_6 \quad (1)$$

The appearance of yellow color followed by orange color indicated the formation of fine nanoscale Cu particles resulting from borohydride-assisted reduction. The reaction was allowed to proceed for 15 min in ambient atmosphere to ensure complete reduction and capping of size-homogeneous Cu NPs. Various optimization studies were performed to investigate the size and shapes of Cu NPs.

Instrumentation and sample preparations

UV-VIS spectroscopy (Perkin Elmer Lambda 35, path length of 1.0 cm, spectral range 200-800 nm, scan rate 1920 nm/sec) was used for preliminary estimation of Cu NPs synthesis. FTIR spectra (Thermo Nicolet 5700) were recorded for centrifuged and nitrogen dried samples of Cu NPs in solid state KBr discs. FTIR spectra provided information about the binding interactions of SDS and Vitamin C with nanosized zero-valant copper particles. Morphological study of the products was carried out with AFM (Agilent 5500) image analysis, for which 250 µg/mL nanoclustor solutions were centrifuged for 1 min and sonicated (KQ 500-DE) for 30 min. ~30 µL aliquots were then extracted and deposited on freshly cleaved mica surfaces for AFM analysis.

TEM (Jeol JEM 1200 EX MKI) images were recorded to confirm size distribution and shape homogeneity of newly synthesized Cu NPs. Samples were prepared by taking small quantities of SDS-capped Cu NPs separated by centrifugation from aqueous solution and re-dispersed in ethanol. These nanoparticles were then mounted on carbon-coated copper grids by dip coating method and vacuum dried in a desiccator for 25 min to ensure complete removal of solvent. XRD (D-8 of Bruker) was carried for phase confirmation and degree of crystallinity of the products. A suitable quantity of Cu NPs sample for XRD analysis was prepared by drying sufficient Cu NPs solution under nitrogen to avoid oxidation. The product thus obtained was washed thoroughly with deionized water and acetone to remove any impurities and un-reacted surfactant and then dried in a pre-heated oven at 100 °C.

Catalytic test for reductive degradation of dye

The catalytic performance of newly synthesized SDS-capped Cu NPs was investigated for reductive degradation of EB dye. The test was performed before and after the addition of Cu NPs catalyst to 100 µM EB with 10 mM $NaBH_4$ to check the reduction/degradation process. The test was carried out in an aqueous solution in quartz cells. UV-Visible spectral changes were recorded to monitor reductive degradation of EB. To investigate the catalytic performance, Cu NPs were first deposited onto pre-weighed glass cover slips, and then dried under inert atmosphere to ensure complete adherence of Cu NPs on the glass surface. The glass cover slips were re-weighed after the deposition of Cu NPs to determine the mass of catalyst. These glass cover slips having the deposit of Cu NPs were placed inside the quartz cell, which already contained the mixture of targeted dye and $NaBH_4$ in aqueous medium.

Results and discussion

Optical characterization

The collective oscillations of conduction electrons at the surface of nanosized metal particles absorb visible electromagnetic waves, the phenomenon is known as SPR **[3]**. This effect can be used to estimate the formation of nanoscale metal particles in the solution medium through simple UV-Vis spectrophotometry. It is worth mentioning that SPR of metal nanoparticles is greatly a size-dependent phenomenon. The electron scattering enhancement at the surfaces of nanoparticles increase bandwidth and decrease the particle size. Hence, variations in bandwidth and shifts in resonance are very important parameters in characterizing the nanosized regime metal particles **[3]**. During the synthesis of SDS-stabilized Cu NPs in aqueous solution, the UV-Visible spectra of selected samples were

recorded at different time intervals, immediately after the addition of $NaBH_4$ and then after 10 and 15 minutes, as depicted in **Fig. 1 (A)**. A yellow/orange color appeared immediately after the addition of $NaBH_4$ with the absence of SPR, shown by dashed line in **Fig. 1 (A)**.

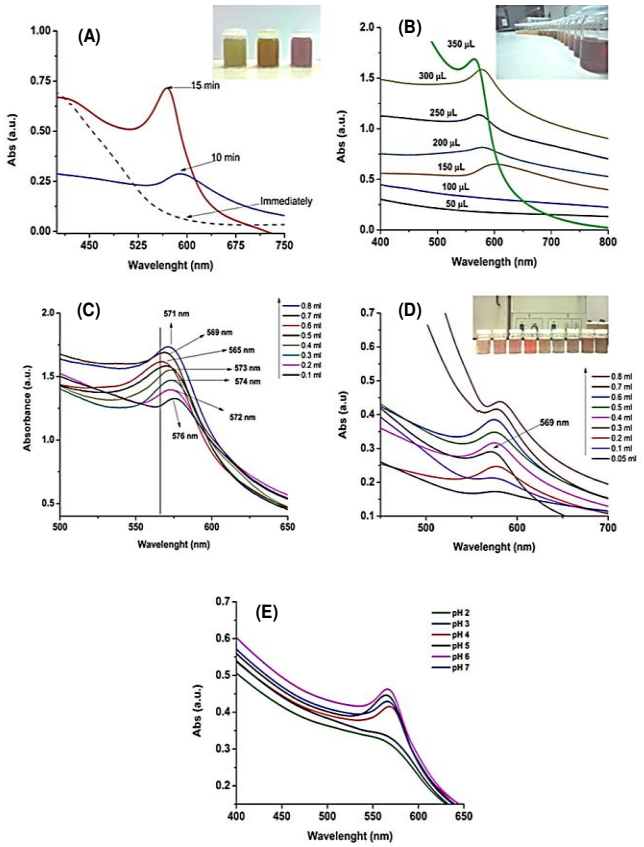

Fig. 1. UV-Vis spectra of Cu NPs synthesized in an aqueous medium, (A) SPR generation of Cu NPs at different time intervals during the reaction and corresponding color change in colloidal sol, shown in inset photograph (B) effect on SPR generation by varying the concentration of reducing agent and corresponding color of Cu NPs (inset photograph) (C) the effect of surfactant concentration on SPR of Cu NPs (D) the effect of precursor salt concentration on SPR generation and color of synthesized Cu NPs (inset photograph) and (E) the shift in SPR position with variation in pH of colloidal Cu NPs.

However, a broad SPR band was generated by the same sample within 10 min of reaction time with maximum absorption around 589 nm, resulting in a purple color of the solution. A brick red color appeared after 15 min together with a highly sharp SPR peak having maximum absorption at 569 nm. These experimental investigations were found to be in very good agreement with the results already presented in the literature **[7]**. Moreover, UV-Vis spectral analysis was carried out for a number of samples prepared in the aqueous medium to optimize parameters such as concentration of precursor salt ($CuCl_2$•$5H_2O$), concentration of reducing agent ($NaBH_4$), effect of pH and reaction time, as depicted in **Fig. 1(B-E)**.

It is obvious that the copper particles with diameters below 4 nm exhibit strong broadening of the Plasmon band **[43]**. It is also evident that the small increase in absorbance (550-600 nm) turn yellow/orange color to red, which indicates the formation of nanoclustor of Zero valent Cu under the influence of reduction reaction **[7]**. The reaction was allowed to continue in air. The solution was kept under an ambient atmosphere for several days to investigate possible oxidation of the formed Cu NPs. Several color tinges appeared with the passage of time and finally the solution was turned into dark green color on the 21st day, indicating the formation of cuprous oxide which was then confirmed by XRD analysis.

Effect of reducing agent on SPR peak position

The formation of Cu NPs was confirmed by the generation SPR with a maximum absorbance at 586 nm. An excess of $NaBH_4$ was required to produce size homogeneity and well-dispersed Cu NPs in colloidal form. Shifts in the SPR band, along with color change, were observed by varying the amount of reducing agent (0.01 M $NaBH_4$) in the volume range of 50-350 µL; the resulting UV-Vis spectra are shown in **Fig. 1(B)**. A blue shift with gradual increase in the absorbance from 597 nm to 569 nm was seen due to the electrostatic interactions between Zero valent Cu NPs **[44]**. There was no clear SPR signal from the yellow colored Cu solution. But a broad and clear peak at 568 nm was observed when the color changed from yellow to orange and also when the reaction mixture gives a brown color (digital photographs inset in **Fig. 1(B)**. This probably confirmed the onset of particle formation. Moreover, with increasing the concentration of reducing agent higher nucleation rates resulted and consequently generated greater number of nanoparticles. Hence, the SPR peak narrowed with increase in absorbance; the phenomenon was also supported by previous studies **[44]**. It was observed that the color changed from light yellow to orange and finally turned brick red, where maximum absorbance was noticed at 569 nm.

Effect of surfactant on SPR peak position

The UV-Vis spectral profile generated for SDS-capped Cu NPs revealed that gradual increase in the concentration of surfactant occurred by varying the volume of 1.0 M SDS from 0.1-0.6 mL. This increase resulted in a blue shift in the SPR position from 576-569 nm and confirms the generation of smaller nano-particles as shown in **Fig. 1(c).** Further increase in the amount of SDS generated a red shift from 569-571 nm indicating the growth of Cu NPs. The red shift in SPR led to gradual increase in the nano-particles size and strong inter-micelle interactions. The higher concentration of surfactant molecules also resulted into potential agglomeration of many small particles of the nanosized regime copper and formed larger spherical particles.

Effect of precursor salt on SPR peak position

UV-Vis spectral lines were recorded for the shift in SPR peak position with variation in the amount (0.05-0.8 mL) of precursor salt, as shown in **Fig. 1(D)**. A blue shift in the wavelength from 577 nm to 569 nm was observed with increase in the amount of precursor salt (0.05 - 0.3 mL of 0.03 M $CuCl_2$•$5H_2O$). This shift can be explained on the basis of increased nucleation rate due to greater amount of Cu (II) ions and generation of smaller nanoparticles in the solution. However, with further increase in the amount of precursor ions, from 0.4 to 0.8 mL, a red shift in the SPR

was observed from 569 nm to 658 nm. This may be due to collision between small nanoparticles, which lead to particle growth **[3]**. The inset digital photo graph in Fig. 1(d) clearly shows the change in color with the size of Cu NPs. A brick red color was noted for the optimal amount of precursor salt producing greatest number of Cu NPs in aqueous medium.

Effect of pH

Solution pH greatly affects the SPR of Cu NPs. The influence of pH on the progress of reduction reaction has also been reported by various scientists **[25**, **28**, **29**, **31**, **32]**. The pH was studied in the range from 2 to 7 with the drop wise addition of 0.1 M NaOH and HCl solutions. Strongly basic medium was avoided to resist the formation of copper oxides **[43]**. The UV-Vis spectral profiles of selected colloidal Cu NPs solutions, prepared under the same experimental conditions except for the pH, are presented in **Fig. 1(E)**. The surface plasmon band for each solution can be seen, except at pH 2 and pH 3. This likely indicated generation of very small particles at such low pH. Plasmon resonance was clearly visible for pH from 4 to7 with measured values of 569 nm, 564 nm, 566 nm and 567 nm respectively. The maximum blue shift in SPR peak position at pH 5 could be attributed to the decrease in particle size compared to nanoparticles prepared at other pH values. The exact position of the SPR band depends on a variety of factors, including size and shape of the particles, nature of the solvent and capping agent **[7]**. In this case, variations in the pH of solution have resulted in different arrangements of the capping molecules around the Cu NPs, which affected the shift in SPR.

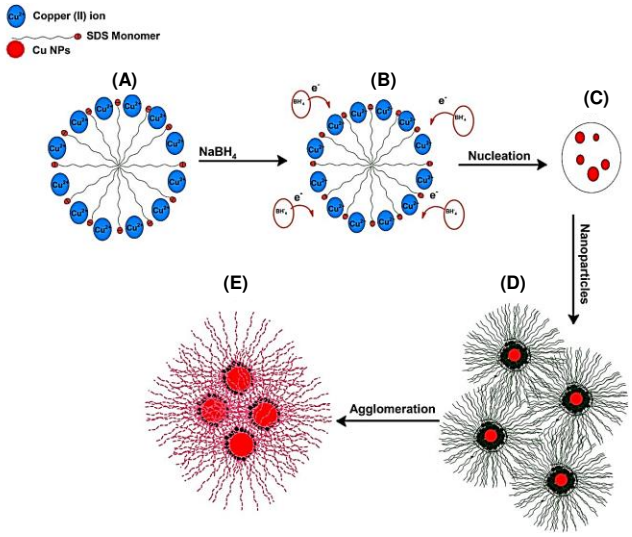

Scheme 1. Mechanism for formation of spherical Cu NPs in aqueous SDS medium.

Mechanism of formation

The mechanism for formation of spherical Cu NPs using SDS as the stabilizing and capping agent in aqueous solution is illustrated in **Scheme 1**. Above the critical micelle concentration (CMC), the aqueous system was densely populated with SDS surfactant micelles. Initially, a large population of copper precursor ions (Cu^{2+}) gathers at the micelle head groups due to electrostatic attraction between the negative surfactant head group and the positively charged copper ions, **scheme 1(A)**.

With the addition of reducing agent ($NaBH_4$), reduction occurs through electron transfer from borohydride anions to copper ions followed by nucleation of copper atoms within the micelle network. These nuclei tend to connect via magnetic dipole interactions resulting in the formation of spherical nanoparticles. The strong micellular effect resists the directional growth of nanoparticles to any other morphology, as explored in **Scheme 1(B-D)**. Conversely, the appearance of aggregated nanoparticles in some regions of TEM images may be due to attractive intermicellular interactions. Such interactions promote micelle growth, and potential agglomeration of micelles to larger spherical particles, as presented in **Scheme 1(E)**.

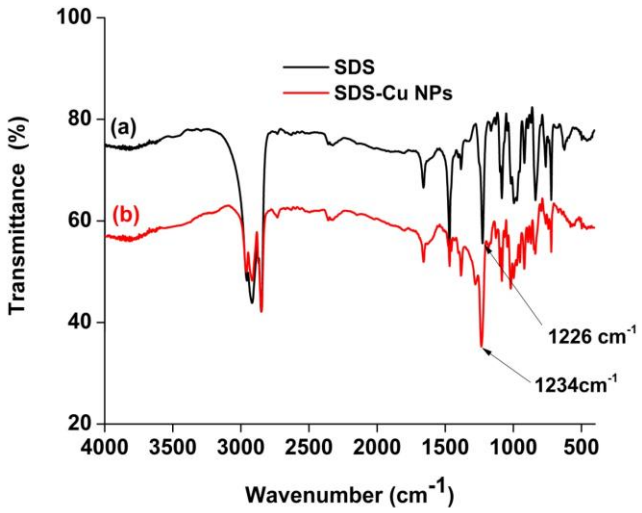

Fig. 2 FTIR spectra, (a) standard SDS surfactant and (b) SDS capped Cu NPs.

Fourier transform infrared spectroscopy

The surface binding interaction study of SDS with Cu NPs was carried out by recording FTIR spectra in the range of 4000-400 cm^{-1}, as shown in **Fig. 2**. The characteristic bands of pure SDS can be divided into two regions, two absorption bands in the range of 2950-2850 cm^{-1}, attributed to the aliphatic group (tail group) and another band at 1226 cm^{-1}, attributed to sulfonic acid (head group) of SDS molecules **[45]**. Moreover, the 1226 cm^{-1} band in pure SDS was blue-shifted to 1234 cm^{-1} in capped Cu NPs. It showed that the capping was due to negatively charged head group moieties. This also reinforces the above mechanism **(Scheme 1)** for formation of Cu NPs. The absence of others prominent bands around 623 cm^{-1}, 588 cm^{-1}, 534 cm^{-1} and 480 cm^{-1}, excluded the possibilities of copper oxides existence, such as Cu_2O and CuO impurities **[46**, **47]**.

Atomic force microscopy

AFM is an important technique for studying the morphology of nanoparticles. Tapping mode AFM imaging was applied to study the SDS-capped Cu NPs. **Fig. 3(A)** shows a typical medium-scale AFM image (0.9 µm × 0.9 µm) of the SDS-capped Cu NPs, where as, **Fig. 3(B)** presents a topographical view of the sample.

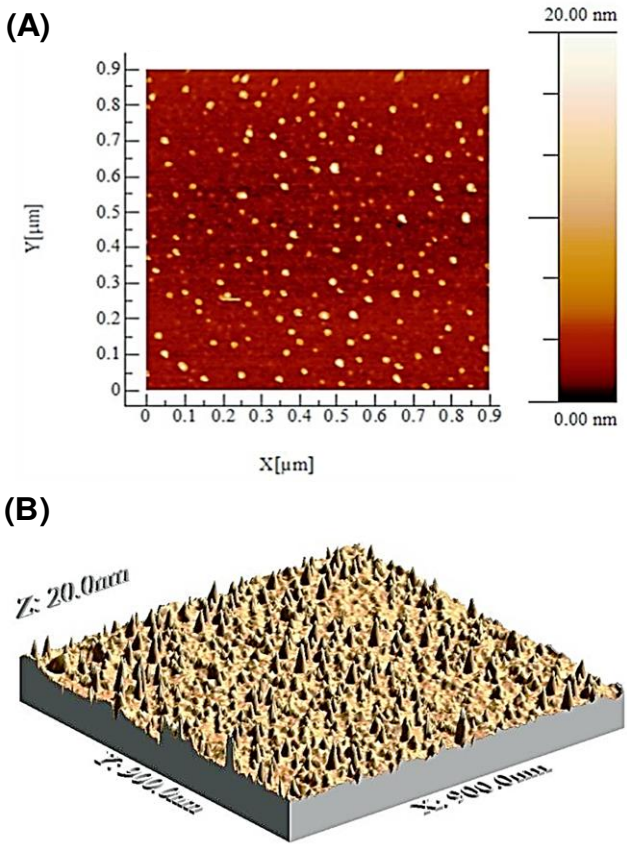

Fig. 3. A typical AFM image of Cu NPs, (A) showing well dispersed and size heterogeneous NPs and (B) 3D topographical map of Cu NPs showing dents and surface irregularities.

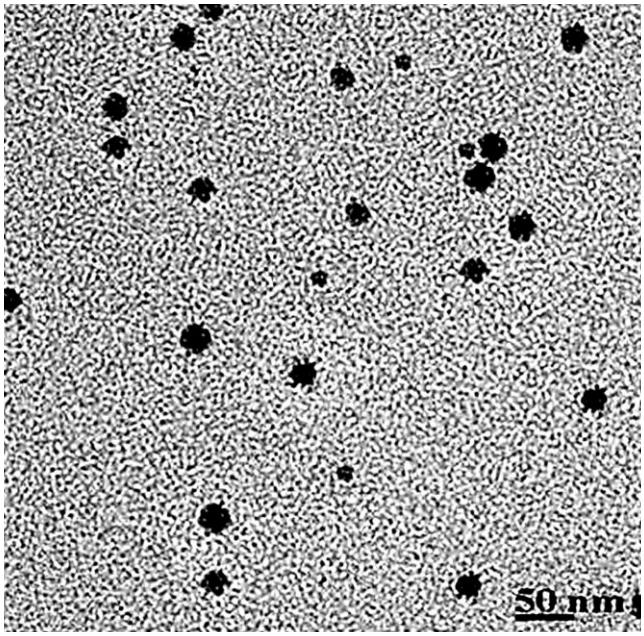

Fig. 4. TEM image of SDS capped Cu NPs showing well distributed NPs with spherical shapes.

The topographic map revealed that the nanoparticles were rich in dents and irregularities on their surfaces. The rough surfaces provide a greater number of active sites and comparatively possess greater surface area than smooth ones; such particles can play a better role in the field of catalysis. Results obtained with AFM identified that newly synthesized Cu NPs possessed an average size of 14 nm. The results acquired for size elucidation using AFM and TEM image analysis were in good agreement.

Transmission electron microscopy

High resolution TEM was used to examine the size and shape of synthesized products. The SDS micelle network was applied as capping agent to get the controlled formation of spherical Cu NPs. This hypothesis was confirmed from TEM image analysis of a selected sample of Cu NPs, as shown in **Fig. 4**. This image confirmed that synthesized Cu NPs were spherical in shape and grown with well-defined morphology. The diameters of these nanoparticles were found to lie in the range between 8 nm to 25 nm, with a mean of 14 nm. In some regions, agglomeration of small nanoparticles was observed which might be caused by interactions of surfactant chains of SDS molecules with each other. The size of Cu NPs was confirmed with TEM and AFM analyses.

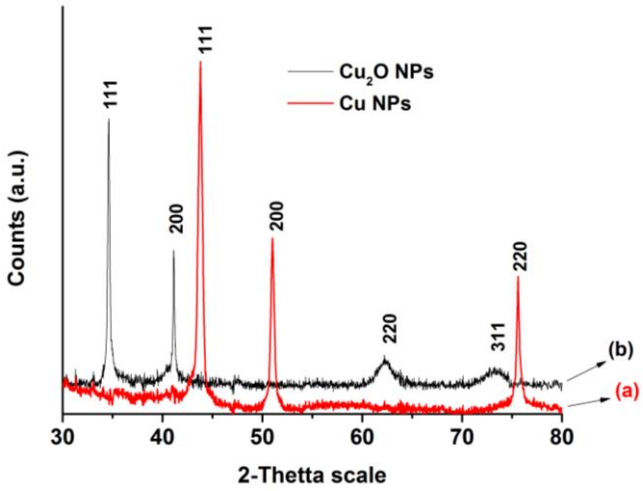

Fig. 5 XRD patterns of the powder samples (a) collected from brick red solution of Cu NPs and (b) collected from greenish suspension of Cu_2O.

X-ray diffraction

The phase composition of crystal structures of the synthesized products, collected from brick red and greenish suspensions of Cu NPs, were analyzed by XRD, as shown in **Fig. 5**. The diffraction data presented in **Fig. 5 (a)** inferred the formation of pure crystalline metallic phase Cu NPs with face centered cubic (FCC) structures having characteristic peaks indexed to (111), (200) and (220) at corresponding 2-theta value of 43.8º, 51.0º and 75.6º respectively. On the other hand, XRD peaks shown in Fig. 5(b) for greenish suspension obtained after 21 days of the synthesis were indexed to cuprous oxide (Cu_2O) with characteristic diffraction indices (111), (200), (220) and (311) at 2-theta value of 34.6º, 41.2º, 62.3º and 73.2º respectively. These results were found in a close relation with the reported work **[47]**.

Catalytic activity

The catalytic activity of SDS-capped Cu NPs was monitored by using EB dye as a test compound. The progression of the catalytic degradation of EB dye can

easily be examined by decrease in optical density at 515 nm, as shown in **Fig. 6(A)**. UV-Vis spectra of EB (100 µM) and $NaBH_4$ (10 mM) mixtures in the absence of Cu NPs showed only a small increase of reductive degradation (up to 14.1%) with time, as shown in **Fig. 6(A)**. The application of others metals nano-particles for the degradation of dyes have also been reported in literature **[42**, **43]**. However, the reductive degradation observed after addition of Cu NPs catalyst in the same sample solutions. The process of degradation of EB dye was completed within 20 sec, as shown in **Fig. 6(B)**. It was also observed that the reaction rate of EB degradation with Cu NPs was enhanced 30 times with 100 % degradation efficiency when compared with the results of the control test.

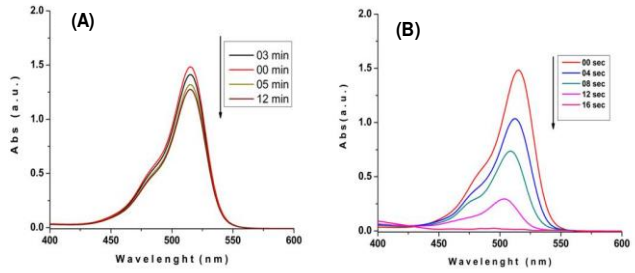

Fig. 6. UV-Vis spectra, (A) 100 µM of EB and 500 µL 0.01 M $NaBH_4$ in absence of nanocatalysts and (B) reduction of 100 µM of EB mixed with 500 µL 10 mM $NaBH_4$ by use of 0.1 mg powder of nanocatalyst (i.e. Cu NPs).

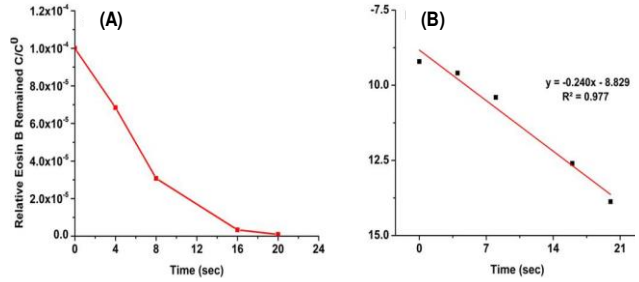

Fig. 7. The amounts remaining of EB, (A) illustrating an exponential decay of the dye and (B) the first order kinetics followed by the reduction/degradation reaction.

The undertaken study explores the extraordinary catalytic behavior of Cu NPs for the degradation of EB dye. The high catalytic activity of Cu NPs may be due to the spherical structure, greater surface active sites from all three dimensions, and rough surface morphology as evident by AFM results. Moreover, well dispersed nature of Cu NPs have the merit of less aggregation providing high surface area per unit volume during the catalytic process.

Kinetic study

UV-Vis spectral results **(Fig. 7)** were used to study the kinetic mechanism of the catalytic reaction. The experiment was carried out by adding 0.1 mg of Cu NPs into 100 µM of EB and 10 mM of $NaBH_4$ in an aqueous medium. The degradation rate of EB was monitored at a maximum wavelength of 515 nm, in the visible region and was found to follow first order kinetics as given by equation (2);

$$\ln\frac{C}{C_o} = -kt \qquad (2)$$

The first order rate constant (k) for degradation of EB was calculated and found 0.240 sec^{-1}, as shown in **Fig. 7(B)**.

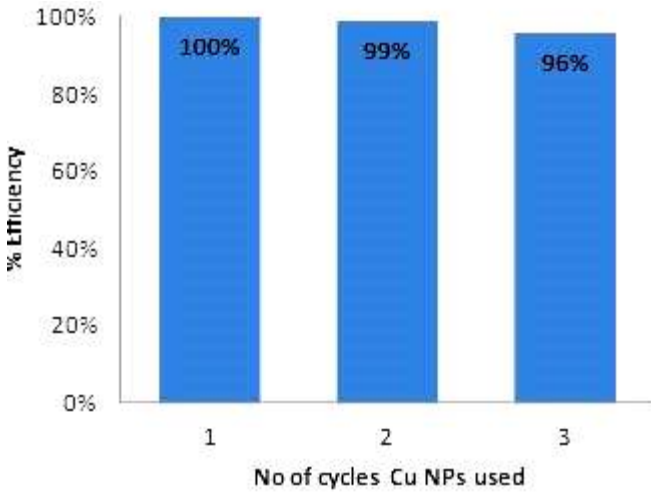

Fig. 8. Recovery of SDS capped Cu NPs three times to carry out reductive degradation of EB dye with negligible loss of catalytic efficiency.

Recovery and reuse of Cu NPs

The newly devised method for synthesis and use of SDS-capped Cu NPs for catalytic reductive degradation of dye, demonstrates simple and effortless recyclability of the nanocatalyst. A bar graph demonstrating the high catalytic efficiency of Cu NPs with triplicate use, as shown in **Fig. 8**. Cu NPs adhered to glass cover slips were used for catalysis and were easily recovered and reused after washing with sufficient quantity of de-ionized water and drying under inert atmosphere. Negligible loss of activity was observed during each recycling.

Conclusion

In the present study, oxidation resistant and stable Cu NPs with narrow and homogenous size distributions were synthesized in aqueous medium without employing any protective gas. The Cu NPs were synthesized using sodium borohydride as a reducing agent, SDS as a capping agent and ascorbic acid (natural vitamin C) was used in capacity of supporting reagent with antioxidant activity. These nanoparticles were employed as recyclable heterogeneous catalysts for ultra-fast reductive degradation of EB dye, which - to the best of our knowledge - has not been addressed previously. Moreover, the study suggests that the synthesis route is free from requirements like high energy, extended preparation time or special equipment. The prepared nanocatalysts can easily be recovered and reused without any significant decline in the efficiency.

Acknowledgements
We acknowledge the Higher Education Commission, Islamabad, Pakistan and the National Centre of Excellence in Analytical Chemistry, University

of Sindh, Jamshoro, Pakistan for provision of financial assistance and facilities during this research.

Reference

1. Tiwari, A.; Shukla, S.K. (Ed.), In Advanced Carbon Materials and Technology, WILEY-Scrivener Publishing LLC, USA, **2014**.
Tiwari, A. *Adv. Mat. Lett*. **2012**, *3*, 1.
DOI: 10.5185/amlett.2012.13001
2. Singh, P.; Katyal, A.; Kalra, R.; Chandra, R. *Tetrahedron Lett*. **2008**, *49*, 727.
DOI: 10.1016/j.tetlet.2007.11.106
Tiwari, A.; Mishra, A. K.; Kobayashi, H.; Turner, A.P.F. (Eds.), In Intelligent Nanomaterials, WILEY-Scrivener Publishing LLC, USA, **2012**.
3. Dang, T.M.D.; T Le, .T.T.; Fribourg-Blanc, E.; Dang, M.C. *Adv. Nat. Sci: Nanosci. Nanotechnol*. **2011**, *2*, 015009.
DOI: 10.1088/2043-6262/2/1/015009
4. Singh, P.; Katyal, A.; Kalra, R.; Chandra, R. *Tetrahedron Lett.* **2008**, *49*, 727.
DOI: 10.1016/j.tetlet.2007.11.106
5. Kim, H.-S.; Dhage, S.; Shim, D.-E.; Hahn, H.T. *Appl. Phys. A*. **2009**, *97*, 791.
DOI: 10.1007/s00339-009-5360-6
6. Lee, J.C.Y.; Lee, K.J.; Stott, N.E.; Kim, D. *Nanotechnology* **2008**, *19*, 415604.
DOI: 10.1088/09574484/19/41/415604
7. Pacheco, M.J.G.; Sánchez, J.E.M.; Hernández, G.; Ruiz, F. *Mater. Lett.* **2010**, *64*, 1361.
DOI: 10.1016/j.matlet.2010.03.029
8. Vaseema, M.; Leeb, K.M.; Kima, D.Y.; Hahna, Y.B. *Mater. Chem. Phys.* **2011**, *125*, 334.
DOI: 10.1016/j.matchemphys.2010.11.007
9. Jushi, S.S.; Pat, S.F.; Iyer, V.; Mahumuni, S. *Nano Struchued Materials*. **1998**, *7*, 1135.
DOI: 10.1016/S0965-9773(98)00153-6
10. Solanki, J.N.; Sengupta, R.; Murthy, Z.V.P. *Solid State Sci*. **2010**, *12*, 1560.
DOI: 10.1016/j.solidstatesciences.2010.06.021
11. Kim, Y.H.; Kang, Y.S.; Lee, W.J. *Mol. Cryst. Liq. Cryst*. **2006**, *445*, 231.
DOI: 10.1080/15421400500366522
12. Liu, Q.; Yasunami, T.; Kuruda, K.; Okido, M. *Transac. Nonfer. Metal. Soc.China*. **2012**, *22*, 2198.
DOI: 10.1016/S1003-6326(11)61449-0
13. Liu, Q.; Yu, R.L.; Qiu, G.Z.; Fang, Z.; Chen, A.L.; Zhao, Z.W. *Transac. Nonfer. Metal. Soc.China*. **2008**, *18*, 1258.
DOI: 10.1016/S1003-6326(08)60213-7
14. Zhu, H.T.; Zhang, C.Y.; Yin, Y.S. *J. Cryst. Growth*, **2004**, *270*, 722.
DOI: 10.1016/j.jcrysgro.2004.07.008
15. Coussy, O.; Chong, T.F. *Comptes Rendus Mécanique.* **2005**, *333*, 507.
DOI: 10.1016/j.crme.2005.01.005
16. Athawale, A.A.; Katre, P.P.; Kumar, M.; Majumdar, M.B. *Mater. Chem. Phy.* **2005**, *91*, 507.
DOI: 10.1016/j.matchemphys.2004.12.017
17. Giuffrida, S.; Costanzo, L.; Ventimiglia, G.; Bongiorno, C. *J. Nanoparticle Research*. **2008**, *10*, 1183.
DOI: 10.1007/s11051-007-9343-2
18. Zhang, H.X.; Siegert, U.; Liu, R.; Cai, W.B. *Nanoscale Res Lett*. **2009**, *4*, 705.
DOI: 10.1007/s11671-009-9301-2
19. Zhang, X.; Yin, H.; Cheng, X.; Hu, H.; Yu, Q.; Wang, A. *Mater. Res. Bull*. **2006**, *41*, 2041.
DOI: 10.1016/j.materresbull.2006.04.008
20. Zhang, X.;Yin, H.; Cheng, X.; Jiang, Z.; Zhao, X.; Wang, A. *Appl. Surf. Sci.* **2006**, 252, 8067.
DOI: 10.1016/j.apsusc.2005.10.010
21. Joshi, S.S.; Patil, S.F.; Iyer, V.; Mahumuni, S. *Nanostruct. Mater.* **1998**, *10*, 1135.
DOI: 10.1016/S0965-9773(98)00153-6
22. Park, B.K.; Jeong, S.; Kim, D.; Moon, J.; Lim, S.; Kim, J.S. *J. Colloid Interface Sci*. **2007**, *311*, 417.
DOI: 10.1016/j.jcis.2007.03.039
23. Zhang, Q.L.; Yang, Z.M.; Ding, B.J.; Lan, X.Z.; Guo, Y.J. *Transactions of Nonferrous Metals Society of China*. **2010**, *20*, 240.
DOI: 10.1016/S1003-6326(10)60047-7
24. Hassan, S.S.; Sirajuddin, Solangi, A.R.; Agheem, M.H.; Junejo, Y.; Kalwar, N.H.; Tagar, Z.A.; *J. Hazard. Mater*. **2011**, *190*, 1030.
DOI: 10.1016/j.jhazmat.2011.04.047
25. Sau, T.K.; Pal, A.; Pal, T. *J. Phys. Chem. B*, **2001**, *105*, 9266.
26. **DOI:** 10.1021/jp011420t
27. Sirajuddin, Mechler, A.; Torriero, A.A.J.; Nafady, A.; Lee, C.Y.; Bond, A.M.; O'Mullaned, A.P.; Bhargavad, S.K. *Coll. Surf. A.* **2010**, *370*, 35.
DOI: 10.1016/j.colsurfa.2010.08.041
28. Sirajuddin, Afridi, H.I.; Shah, S.S.; Niaz, A. *J. Iran. Chem. Soc*, **2011**, *8*, 34.
DOI: 10.1007/BF03254280
29. Huanga, J.H.; Zhou, C.F.; Zenga, G.M.; Li, X.; Niu, J.; Huang, H.J.; Hea, L.J.S.S.B. *J. Membr. Sci*. **2010**, *365*, 138.
DOI: 10.1016/j.memsci.2010.08.052
30. Martína, J.S.; elasco, M.G.; Heredia, J.B.; Carvajal, J.G.; Fernández, J.S. *J. Hazard. Mater*. **2010**, *174*, 9.
DOI: 10.1016/j.jhazmat.2009.09.008
31. Rauf, M.A.; Meetani, M.A.; Hisaindee, S. *Desalination*, **2011**, *276*, 13.
DOI: 10.1016/j.desal.2011.03.071
32. Sun, Z.; Chen, Y.; Ke, Q.; Yang, Y.; Yuan, J. *J. Photochem. Photobiol. A*. **2002**, *149*, 169.
DOI: 10.1016/S1010-6030(01)00649-9
33. Tanak, K.; Padermpole, K.; Hisanga, T. Water Res. **2000**, *34*, 327.
DOI: 10.1016/S0043-1354(99)00093-7
34. Konstantinou, I.K.; Albanis, T. A. *Appl. Catal. B*, **2004**, *49*, 1.
DOI: 10.1016/j.apcatb.2003.11.010
35. Zuas, H.B.O.; Hamim, N.; *Adv. Mat. Lett*. **2013**, *4*, 662.
DOI: 10.5185/amlett.2012.12490
36. Tanmay, P.D.; Ghorai, K. *Adv. Mat. Lett*. **2012**, *4*, 121.
DOI: 10.5185/amlett.2012.7382
Imani, R.; Iglič, A.; Turner, A.P.F.; Tiwari, A. *Electrochemistry Communications*, **2014,** 40, 84-87.
37. Janus, M.; Morawski, A.W. *Appl. Catal. B* **2007**, *75*, 118.
DOI: 10.1016/j.apcatb.2007.04.003
38. Wawrzyniak, B.; Morawski, A.W. *Appl. Catal. B* **2007**, *62*, 150.
DOI: 10.1016/j.apcatb.2005.07.008
39. Xiong, Y.; Karlsson, H.T. *J Environ Sci Health A Tox Hazard Subst Environ Eng*. **2001**, *36*, 321.
DOI: 10.1081/ESE-100102925
40. Appleton, E.L. *Environ. Sci. Technol*. **1996**, *30*, 536.
DOI: 10.1021/es962526i
41. Kalwar, N.H.; Sirajuddin, Sherazi, S.T.H.; Khaskheli, A.R.; Hallam, K.R.; Scott, T.B.; Tagar, Z.A.; Hassan, S.S.; Soomro, R.A. *Appl. Catal. A*. **2013**, *453*, 54.
DOI: 10.1016/j.apcata.2012.12.005
42. Bokare, A.D.; Chikate, R.C.; Rode, C.V.; Paknikar, K.M. *Appl. Catal. B*. **2008**, *79*, 270.
DOI: 10.1016/j.apcatb.2007.10.033
43. Jiang, Z.J.; Liu, C.Y.; Sun, L.W. *J. Phys. Chem. B*, **2005**, *109*, 1730.
DOI: 10.1021/jp046032g
44. Hossain, S.; Fatema, U.K.; Mollah, M.Y.A.; Rahman, M.M.; Susa, M.A.B.H. *J. Bangl. Chem. Soc*. **2012**, *25*, 71.
DOI: 10.3329/jbcs.v25i1.11777
45. De, S.; Mandal, S. *Colloids Surf. A* **2013**, *421*, 72.
DOI: 10.1016/j.colsurfa.2012.12.035
46. Taffarel, S.R.; Rubio, J. *Miner. Eng*. **2010**, *23*, 771.
DOI: 10.1016/j.mineng.2010.05.018
47. Kooti, M.; Matouri, L. *Transac. F: Nanotech*. **2010**, *17*, 73.
48. Tian, K.; Liu, C.; Yang, H.; Ren, X. *Colloids Surf. A* **2012**, *397*, 12.
DOI: 10.1016/j.colsurfa.2012.01.019.

